

Soft Matter

Accepted Manuscript



This is an *Accepted Manuscript*, which has been through the Royal Society of Chemistry peer review process and has been accepted for publication.

Accepted Manuscripts are published online shortly after acceptance, before technical editing, formatting and proof reading. Using this free service, authors can make their results available to the community, in citable form, before we publish the edited article. We will replace this *Accepted Manuscript* with the edited and formatted *Advance Article* as soon as it is available.

You can find more information about *Accepted Manuscripts* in the [Information for Authors](#).

Please note that technical editing may introduce minor changes to the text and/or graphics, which may alter content. The journal's standard [Terms & Conditions](#) and the [Ethical guidelines](#) still apply. In no event shall the Royal Society of Chemistry be held responsible for any errors or omissions in this *Accepted Manuscript* or any consequences arising from the use of any information it contains.



Cite this: DOI: 10.1039/xxxxxxxxxx

The relation between local density and bond-orientational order during crystallization of Gaussian core model[†]

Yan-Wei Li^{ac} and Zhao-Yan Sun^{ab*}

Received Date

Accepted Date

DOI: 10.1039/xxxxxxxxxx

www.rsc.org/journalname

Whether the nucleation is triggered by density or by bond-orientational order is one of the most hot-debated issues in recent investigations of the crystallization process. Here, we present a numerical study of the relation between them for soft particles in the isothermal-isobaric ensemble. We compress the system and thus obtain the fluid-solid transition. By investigating locally dense-packed particles and particles with relatively high bond-orientational order in the compressing process, we find sharp increases of the spatial correlations for both densely packed particles and highly bond-orientational ordered particles at the phase transition point, which provide new characterization methods of the liquid-crystal transition. We also find that it is the bond-orientational order rather than density that triggers the nucleation process. The relation between local density and bond-orientation order parameter is strongly affected by the characterization methods used. The local bond order parameter (q_6) shows clear correlation with the local density (ρ) in the fluid stage, while the coarse-grained form (\bar{q}_6) does not correlate with ρ at all, owing to the comparable spatial scales of q_6 and ρ . Nevertheless, \bar{q}_6 shows obvious advantage in distinguishing between solid and liquid particles in our work. These results may elevate our understanding of the mechanism of the crystallization process.

1 Introduction

Crystallization is an important process in both condensed-matter physics and technology.^{1–3} The liquid-crystal transition of a system is normally accompanied with the evolution of both bond-orientational order and density. Although this process is well known on the qualitative level, the understanding of it in microscopic detail is still far and seems to be quite complex.

The classical nucleation theory (CNT),^{4,5} which is the first phenomenological description of the nucleation mechanism, provides a concrete physical picture of the nucleation process. It asserts that the crystallization occurs via the formation and subsequent growth of nuclei through spontaneous thermal fluctuation. The initial supercooled liquid phase is considered as a uniform back-

ground, and the nuclei can be formed at any location in it with equal probability. Due to the free-energy barrier to cross, the nuclei can grow only when the size of nuclei exceeds the critical nucleus size, accompanied with the variation of both bond-orientational order and density simultaneously, which is named as one-step nucleation mechanism.

Recent works have shown that there are some other scenarios of the crystallization beyond the above picture. ten Wolde and Frenkel suggested that the locally dense liquid structures serve as precursors of nuclei, which can greatly reduce the free energy barrier and enhance the crystallization rate.⁶ This density controlled two-step nucleation process has been confirmed in theoretical,^{7,8} simulational,^{9–11} and experimental¹² works. However, recent works have shown another kind of precursor, i.e., particles with relatively high bond-orientational order play more important role in the nucleation process.^{13–17}

The above two-step scenarios provide different processes of nucleation. Since both density and bond-orientational order proceed in the crystallization process, it is necessary to know whether there is any correlation between them. Previous works have shown that the local density and bond-orientational order are decoupled with each other and the latter plays a more important role in the nucleation process.^{14,15} However, the characterization

a State Key Laboratory of Polymer Physics and Chemistry, Changchun Institute of Applied Chemistry, Chinese Academy of Sciences, Changchun 130022, China.

b Xinjiang Laboratory of Phase Transitions and Microstructures in Condensed Matters, College of Physical Science and Technology, Yili Normal University, Yining, 835000, China

c Dutch Polymer Institute (DPI), PO Box 902, Eindhoven, 5600 AX, The Netherlands.

* E-mail: zysun@ciac.ac.cn

† Electronic Supplementary Information (ESI) available: Results for the Lennard-Jones system are consistent with main conclusions of Gaussian core model. See DOI: 10.1039/b000000x/

of the bond-orientational order used in these works is the coarse-grained local bond order parameters \bar{q}_6 , which contains the information of the position of both the first shell around the target particle and the second shell around it. On the other hand, the local density ρ , which is calculated from the Voronoi volume v of each particle, contains only the information of the local structure of the first shell around the target particle. Thus, these two quantities characterize the local properties in different spatial scales. This mismatching may introduce some uncertainties to the obtained results. Up to now, the relation between the local density and bond-orientational order still remains elusive, and which quantity plays a primary role during crystallization is unclear.

In this paper, we study the relation between local density and bond-orientational order in the crystallization process for soft particles by using molecular dynamics (MD) simulation in the isothermal-isobaric ensemble. We show that the fluid-solid transition can be attained by simply compressing the system. By investigating the spatial correlation of the locally dense-packed particles and that of highly bond-orientational ordered particles in the compressing process, we find sharp increase in these two kinds of correlations at the phase transition point, indicating that both of them can be used as the characterization methods of the liquid-crystal transition. We then focus on the crystallization process at the phase transition point and show that it is bond-orientational order rather than density that triggers the nucleation process. The correlation between local density and bond-orientational order is strongly influenced by the characterization methods used. q_6 shows clear correlation with ρ in the fluid phase, which is probably due to the comparable characterizing spatial scales of q_6 and ρ , while \bar{q}_6 does not correlate with ρ at all. Moreover, we find that the correlation between local density and bond-orientational order shows clear crystal fraction dependence. Nevertheless, \bar{q}_6 shows obvious advantage in distinguishing between solid and liquid particles in our work. The above findings may provide more insight into the understanding of the microscopic details of the crystallization process.

2 Methods

2.1 Model and simulation details

We perform MD simulation in the isothermal-isobaric ensemble using the GALAMOST software package.¹⁸ The temperature T and the pressure P are maintained by the Nosé-Hoover thermostat^{19,20} and Andersen barostat,²¹ respectively. Our systems consist of $N = 13500$ particles in the three dimensional (3D) simulation box with periodic boundary conditions. Particles interact via the Gaussian-shaped potential, which is originally introduced by Stillinger.²²

$$V(r) = \varepsilon \exp\left(-\frac{r^2}{\sigma^2}\right), \quad (1)$$

where ε and σ characterize the energy and length scales, respectively. In this work, we set $\varepsilon = 1$, $\sigma = 1$ and the Boltzmann constant $k_B = 1$. The cutoff in the interaction is set to $r_c = 3.7$. The so-called Gaussian-core model (GCM), is a typical representative of a class of systems of interpenetrating particles,^{22–24} and it is a good model for various soft materials, such as star-polymers

and dendrimers.²⁵ Since particles interact via bounded and weak potential, there is a maximum freezing temperature T_{max} in this system, and the phase diagram exhibits two distinctive features, i.e., above T_{max} the fluid phase is stable at all densities and below T_{max} the system undergoes reentrant melting into a dense fluid phase.^{26–31}

The particles are initially placed randomly in the simulation box, and the system is melted at $T = 0.0052$ and $P = 0.005$ in the fluid phase. The stable body-centered cubic (bcc) and face-centered cubic (fcc) phases can be obtained by simply compressing the system at different temperatures.³¹ We compress the system along two pathways according to the reported phase diagram of GCM^{26–31} (just called bcc compressing line and fcc compressing line for convenience). For the bcc compressing line, we compress the system from $P = 0.01$ to $P = 0.06$ at $T = 0.0052$ by an interval of 0.005. For the fcc compressing line, we compress the system from $P = 0.002$ to $P = 0.011$ at $T = 0.00262$ by an interval of 0.001. In each interval, 2.0×10^7 and 1.0×10^7 time steps are used to equilibrium and sample, respectively. In the following we will indicate the different state points just by their temperature and pressure. To investigate the nucleation process, we track the whole trajectory of every particle at the phase transition point.

2.2 Structure analysis

To characterize the bond-orientational order of particles, we measure its local bond order parameters,^{32–34}

$$q_l(i) = \left(\frac{4\pi}{2l+1} \sum_{m=-l}^l |q_{lm}(i)|^2 \right)^{1/2}, \quad (2)$$

here

$$q_{lm}(i) = \frac{1}{N_b(i)} \sum_{j=1}^{N_b(i)} Y_{lm}(\mathbf{r}_{ij}), \quad (3)$$

where $N_b(i)$ is the number of nearest neighbors of particle i . The neighbors of each particle are determined by the Voronoi method.³⁵ $Y_{lm}(\mathbf{r}_{ij})$ is the spherical harmonic function with degree l and order m , and \mathbf{r}_{ij} is the vector from particle i to particle j . To identify solid-like particles, q_{6m} is normalized,

$$d_{6m}(i) = \left(\frac{q_{6m}(i)}{\left(\sum_{m=-6}^6 |q_{6m}(i)|^2 \right)^{1/2}} \right), \quad (4)$$

Using the set of normalized complex vectors d_{6m} , one can then define the scalar product

$$S_{ij} = \sum_{m=-6}^6 d_{6m}(i) d_{6m}^*(j), \quad (5)$$

which measures the correlation between the structures surrounding particles i and j . * indicates complex conjugation. Two particles i and j are defined to be *connected* if $S_{ij} > 0.6$. Particle i is then defined as solid if it has at least $\xi = 9$ *connected* neighbors (ξ is called the solid bond number).^{13,31,33}

Another set of bond order parameters,

$$W_l(i) = \sum_{m_1+m_2+m_3=0}^l \binom{l}{m_1 \ m_2 \ m_3} \frac{q_{lm_1}(i)q_{lm_2}(i)q_{lm_3}(i)}{(\sum_{m=-l}^l |q_{lm}(i)|^2)^{3/2}}, \quad (6)$$

where the term in parentheses is the Wigner $3j$ symbol, which is nonzero only when $m_1 + m_2 + m_3 = 0$. To further identify the solid-like particles, we adopt the following criterion for crystal classification:^{32–34} (i) bcc particles are all crystal particles with $W_6 > 0$; (ii) fcc particles are all crystal particles with $W_6 < 0$ and $W_4 < 0$; (iii) hcp particles are all crystal particles with $W_6 < 0$ and $W_4 > 0$.

$q_l(i)$ can be further coarse-grained over all the neighbors to obtain $\bar{q}_l(i)$ ³⁶

$$\bar{q}_l(i) = \left(\frac{4\pi}{2l+1} \sum_{m=-l}^l |\bar{q}_{lm}(i)|^2 \right)^{1/2}, \quad (7)$$

with

$$\bar{q}_{lm}(i) = \frac{1}{N_c(i)} \sum_{k=0}^{N_c(i)} q_{lm}(k), \quad (8)$$

here the sum from $k = 0$ to $N_c(i)$ runs over the particle i itself plus the neighboring particles which are in the same phase (liquid or solid) as particle i . The above definitions indicate that $q_l(i)$ holds the information of the structure of the first shell around particle i , and its coarse-grained form $\bar{q}_l(i)$ takes the first and the second shells into account. Recent work suggested that \bar{q}_l is a more effective tool to distinguish different crystal structures than q_l .³⁶

3 Results and discussion

In this section, we first provide the pressure evolution of some static properties in the compressing process. Then we mainly concentrate on the relation between local density and bond-orientational order and their roles in the crystallization process.

3.1 P dependence of some static properties in the compressing process

We first investigate the change of static structure of the system during compressing. In Fig. 1(a), we show the typical curves of the radial distribution functions (RDF) at different pressures for $T = 0.0052$ and $T = 0.00262$. RDF can be used to analyze the pair structures and the long-range order of the system, and distinguish the main structures of the resulting crystals. From the evolution of the RDF during compressing, we can see that the structure of the system is liquid-like at lower pressures ($P < 0.05$ for $T = 0.0052$ and $P < 0.01$ for $T = 0.00262$) and crystallizing at higher pressures. The phase transition point locates at around $P = 0.05$ for $T = 0.0052$ and $P = 0.01$ for $T = 0.00262$, respectively. The structure of the system for $T = 0.0052$ is mainly bcc and that for $T = 0.00262$ is mainly fcc after crystallization, which can be seen from the peak positions of the RDF. Fig. 1(b) and Fig. 1(c) show the probability distribution of W_6 and W_4 , respectively. As has been discussed in the previous section, W_6 can be used to distinguish bcc crystals from those close-packed crystals (fcc and hcp), and W_4 can be used to distinguish fcc crystals

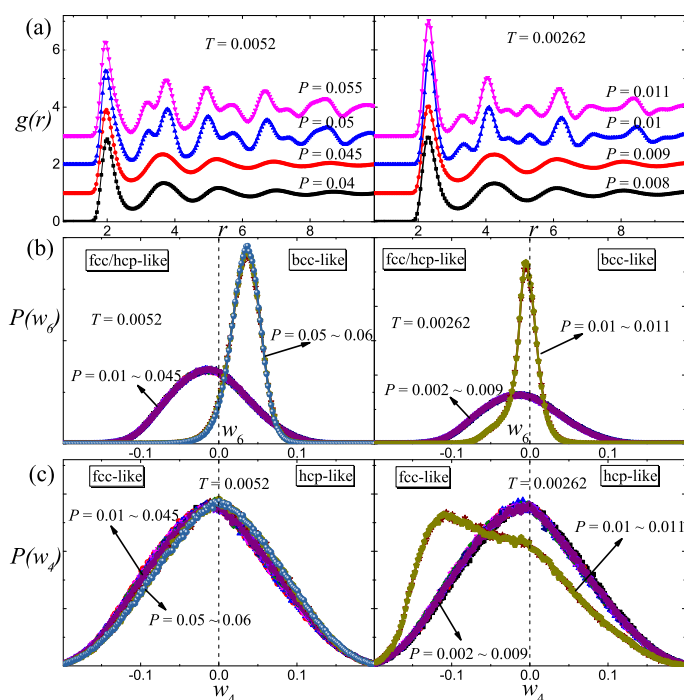


Fig. 1 (a) The radial distribution functions, (b) W_6 probability distribution and (c) W_4 probability distribution at different pressures for $T = 0.0052$ (left) and $T = 0.00262$ (right). The results for RDF have been shifted for clarity.

from hcp crystals. Consistent with the above RDF results, the system goes through the fluid-like phase at lower pressures and the crystal phase (mainly bcc crystal at $T = 0.0052$ and fcc crystal at $T = 0.00262$) at higher pressures for the two compressing lines we investigate. Our results are also consistent with the previous predictions of the phase diagram of GCM,³¹ indicating the crystal structures formed at different state points are mainly determined by the free energy of the system.

The RDF is the statistical average of the two-body correlation over the whole system, but it is hard to describe the detailed local structural information of the system. A good candidate to characterize the local structural environment is the local density ρ ($\rho = 1/v$, where v is the Voronoi volume). Fig. 2(a) shows the probability distribution functions of v at different pressures for the bcc compressing line (the results are similar for the fcc compressing line). It can be seen that the distributions of the Voronoi volume become higher and narrower and shift towards lower values as increasing the pressure of the system. This indicates that the system becomes denser as compressing, resulting in denser local structural environment of particles. Following the method proposed by Starr et al.³⁷, we investigate the statistical properties of the Voronoi cells by calculating the scaled distribution of v . In Fig. 2(b), v is shifted by the average Voronoi volume $\langle v \rangle$ and then normalized by the standard deviation σ_v ($\sigma_v^2 = \langle v^2 \rangle - \langle v \rangle^2$). The scaled distributions collapse to a universal curve when $P > 0.01$, but break down at around $P = 0.01$, which is probably owing to the system entering into the gas state or dilute liquid state at low pressure. Our result is quite consis-

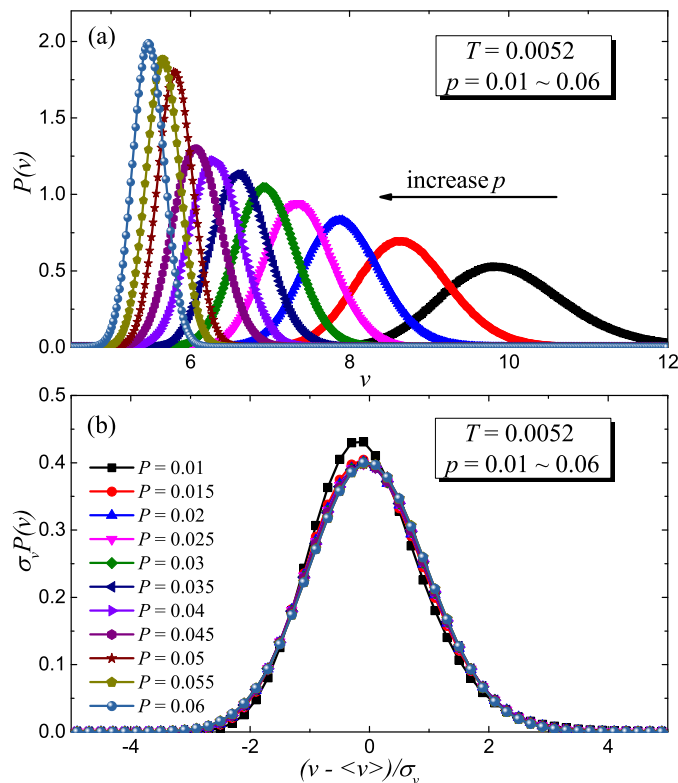


Fig. 2 (a) The probability distribution of the Voronoi volume v at different pressures for $T = 0.0052$. The results have been scaled so that the area of each curve is equal to 1. (b) Scaled distribution of Voronoi cell volumes, $\sigma_v P(v)$ as a function of the normalized Voronoi volume, $((v - \langle v \rangle)/\sigma_v)$ at different pressures for $T = 0.0052$.

tent with the polymer glass system, in which the scaling collapse is expected to be universal in liquid state, but not in the ideal gas phase.³⁷ Moreover, previous works show the similar collapse holds in jammed systems³⁸ but deviates in soft-potential colloidal suspensions³⁹. These findings^{37–39} and our results show that the scaling collapse of the Voronoi volume is likely to be hold in dense liquid and solid, but not holds in gas and dilute liquid. The holding of this scaling behavior may suggest the existence of similar geometric structure of the first coordination shell for particles of the system.

The above Voronoi volume only characterizes the first coordination shell local geometry, which is in a rather small spatial scale. Another intriguing question is whether differences between dense liquid phase and solid phase can be distinguished by some structural characterizations in a larger spatial scale. We further compare the spatial correlation of the locally dense-packed structural environment with that of the locally bond-orientational ordered structural environment, we define 13% of particles with the largest ρ and 13% of particles with the largest q_6 as the locally dense-packed particles and the locally highly bond-orientational ordered particles, respectively (the qualitative results are not sensitive to the choice of the threshold value 13%). Two densely packed particles (or two highly bond-orientational ordered particles) are considered to belong to the same cluster if they are neighbors defined by the Voronoi method. The number of densely

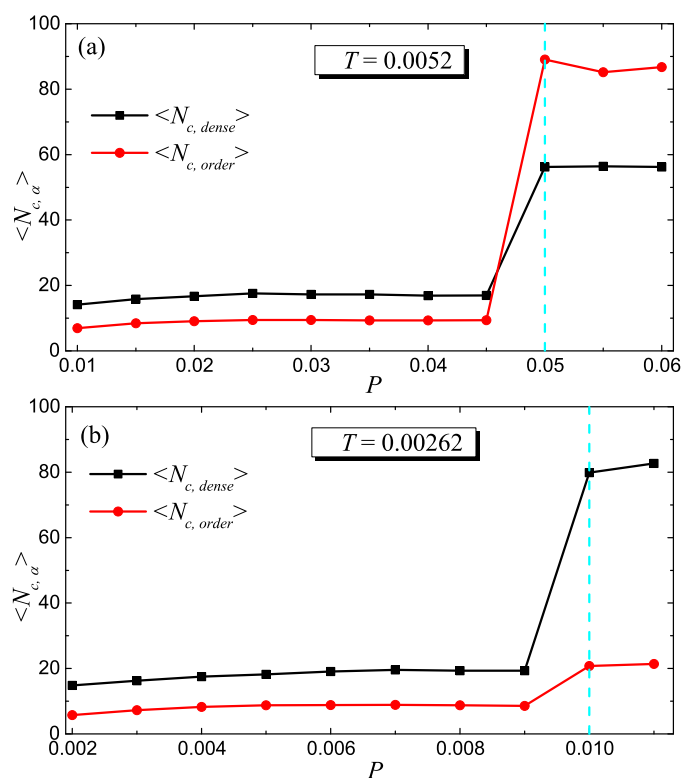


Fig. 3 Pressure dependence of the number averaged cluster size $\langle N_{c,dense} \rangle$ and $\langle N_{c,order} \rangle$ for $T = 0.0052$ (a) and $T = 0.00262$ (b). Throughout compressing the system, sharp increases in $\langle N_{c,dense} \rangle$ and $\langle N_{c,order} \rangle$ can be seen in both (a) and (b), signifying a first-order phase transition (marked by the cyan dashed line).

packed particles (or the highly bond-orientational ordered particles) that are belonging to a cluster is defined as the single cluster size $N_{c,\alpha}$. Here the subscript $\alpha = dense$ is for densely packed particles and $\alpha = order$ is for highly bond-orientational ordered particles. The number averaged cluster size $\langle N_{c,\alpha} \rangle$ is defined as

$$\langle N_{c,\alpha} \rangle = \frac{\sum_{N_{c,\alpha}=1}^{\infty} N_{c,\alpha} P(N_{c,\alpha})}{\sum_{N_{c,\alpha}=1}^{\infty} P(N_{c,\alpha})}, \quad (9)$$

where $P(N_{c,\alpha})$ is the probability of finding a single cluster size $N_{c,\alpha}$, and $\sum_{N_{c,\alpha}=1}^{\infty} P(N_{c,\alpha}) = 1$. The value of $\langle N_{c,\alpha} \rangle$ reflects the spatial correlation of the quantity α .

In Fig. 3, we show the pressure dependence of $\langle N_{c,dense} \rangle$ and $\langle N_{c,order} \rangle$ for both $T = 0.0052$ and $T = 0.00262$. When pressures are lower than the liquid-crystal transition point ($P = 0.05$ for $T = 0.0052$ and $P = 0.01$ for $T = 0.00262$, as can be seen from Fig. 1), the values of $\langle N_{c,dense} \rangle$ and $\langle N_{c,order} \rangle$ are both small. $\langle N_{c,dense} \rangle$ are larger than $\langle N_{c,order} \rangle$ at all state points in the fluid phase for both $T = 0.0052$ and $T = 0.00262$, which suggests that the spatial correlation of densely packed particles is stronger than that of the highly bond-orientational ordered particles in the fluid phase. Moreover, sharp increases both occur for $\langle N_{c,dense} \rangle$ and $\langle N_{c,order} \rangle$ at the liquid-crystal transition point (the position of cyan dashed lines in Fig. 3), indicating the existence of the first-order phase transition. This phase transition point is exactly consistent with our previous RDF and W_6 results. On the other

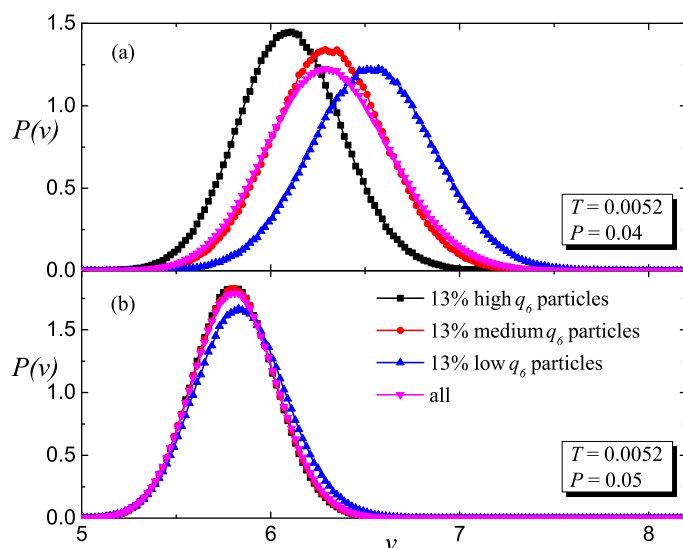


Fig. 4 The probability distributions of the Voronoi volume ν for particles with different degrees of bond-orientational order at $P = 0.04$ (a) and $P = 0.05$ (b) for $T = 0.0052$. Different symbols are for particles with different q_6 , and the legends are shown in (b). The results have been scaled so that the area of each curve is equal to 1.

hand, $\langle N_{c,dense} \rangle$ is smaller than $\langle N_{c,order} \rangle$ for bcc-favored solid phase (see Fig. 3(a)), while greater than $\langle N_{c,order} \rangle$ for fcc-favored solid phase (see Fig. 3(b)). We have tested the Lennard-Jones (LJ) system, in which the favored solid phase is also fcc (see Fig. S1 in the ESI[†]). Consistent with Fig. 3(b), $\langle N_{c,dense} \rangle$ is larger than $\langle N_{c,order} \rangle$ in the solid phase of LJ system (see Fig. S2 in the ESI[†]), which implies that the values of $\langle N_{c,dense} \rangle$ and $\langle N_{c,order} \rangle$ are quantitatively affected by the structure of different polymorphs in the solid phase. Nevertheless, $\langle N_{c,dense} \rangle$ and $\langle N_{c,order} \rangle$ can still be used as benchmarks to characterize the liquid-crystal phase transition, at least for the systems we studied.

Next, we investigate the relation between local density and bond-orientational order in the fluid phase and in the crystal phase as compressing the system. We sort all particles according to their values of q_6 , then we calculate the probability distributions of the Voronoi volume ν for three parts of particles with different degrees of bond-orientational order (i.e., 13% high q_6 particles, 13% medium q_6 particles and 13% low q_6 particles). Figs. 4(a) and 4(b) show these three distributions together with that for all particles in the fluid phase and in the crystal phase, respectively. In the fluid phase ($P = 0.04$), the distributions shift to lower ν as q_6 increased, which indicates that particles with high bond-orientational order are more likely to be densely packed ones, and vice versa. Besides, the distribution curve of ν for the 13% medium q_6 particles is very close to that for all particles. This is reasonable since the distribution for all particles is averaged over particles with different q_6 and this leads to the obtained moderate results. On the other hand, the distribution curves of ν for particles with different q_6 are very close with each other in the crystal phase ($P = 0.05$), although slight differences exist for the curve of particles with low q_6 , which is because particles with stacking faults and liquid-like particles exist in the system. This implies

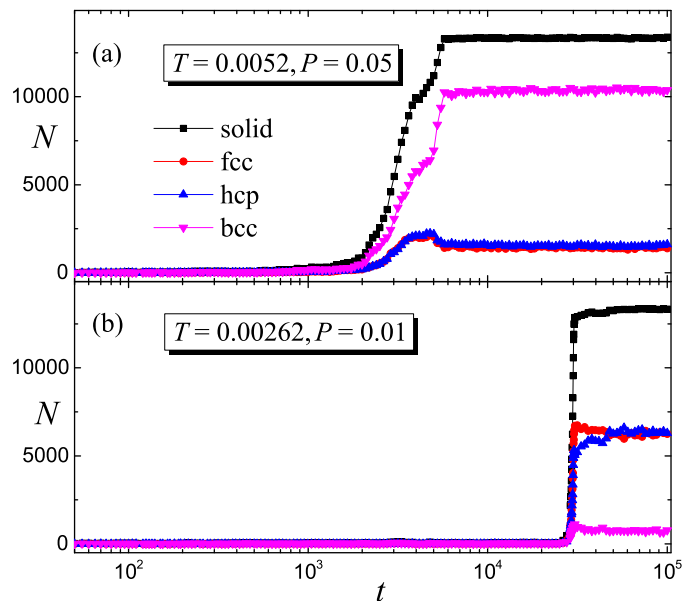


Fig. 5 Time evolution of the number of solid particles and that of different polymorphs (fcc, hcp and bcc) for $T = 0.0052$ (a) and $T = 0.00262$ (b). Different symbols represent different types of particles.

that the local density and the bond-orientational order have little correlation with each other in the crystals with different polymorphs.

3.2 The relation between local density and bond-orientational order during crystallization at phase transition points

From above discussion, we know that both $\langle N_{c,dense} \rangle$ and $\langle N_{c,order} \rangle$ increase sharply at the liquid-crystal transition point, implying that $\langle N_{c,dense} \rangle$ and $\langle N_{c,order} \rangle$ may be coupled during crystallization. However, the probability distributions of the Voronoi volume (Fig. 4(b)) suggest little correlation between local density and bond-orientational order in crystal-state. In order to illustrate the relation between local density and bond-orientational order in detail, we give a further investigation on the structure change during nucleation and growth stages in the crystallization process. We track the whole trajectory of each particle at the phase transition points for both bcc and fcc compressing lines. Fig. 5 shows the time evolution of the number of total solid particles and the number of particles with fcc, hcp or bcc structure for the two state points. Clearly, both systems are in the fluid state initially. There are few solid particles in each system at this stage, and the duration of this stage depends on the initial configuration and the thermal fluctuation of the system. At some time points, the size of nuclei exceeds the critical value, and then the number of solid particles grows in a rapid rate until the whole system crystallizes. At the end of this nucleation/growth stage for $T = 0.0052$ and $P = 0.05$, the number of fcc and hcp particles decreases from their peak values while the number of bcc particles keeps increasing, indicating that some fcc and hcp particles transform into bcc particles in the late stage of crystallization. Similar phenomenon occurs for the state point $T = 0.00262$ and

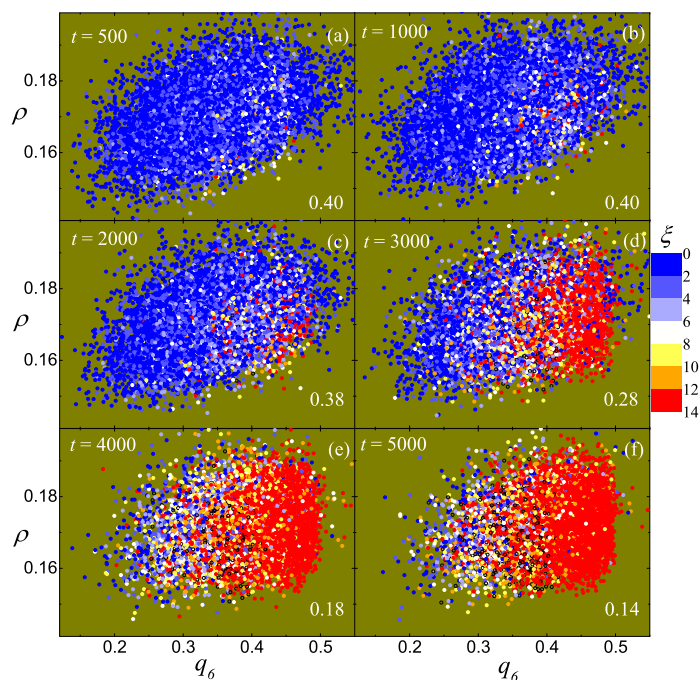


Fig. 6 Time evolution of the solid bond number ξ for all particles of the system in the q_6 - ρ plane for the state point $T = 0.0052$ and $P = 0.05$. Here, ξ grows from 0 to 14 from the liquid to the crystal phase and is represented by the color of each symbol. Numbers at the lower right of each histogram indicate Spearman rank correlation coefficients $K(\rho, q_6)$, which characterizes the correlation between ρ and q_6 . The time for each histogram is shown at the top left of each one.

$P = 0.01$, and there are some bcc and fcc particles transform into hcp structure in the late stage of crystallization. We infer that this is the self-adjusting of the system in order to lower the free energy. Similar results are also found in other recently published works.^{15,31,40} Moreover, bcc phase is the dominant phase at the state point $T = 0.0052$ and $P = 0.05$ and close-packed phases (hcp and fcc) are the dominant ones at the state point $T = 0.00262$ and $P = 0.01$. The former is consistent with while the latter is different from ref.³¹ In Tanaka's work,³¹ it is found that bcc phase is also the dominant one for the state point $T = 0.00262$ and $P = 0.01$. This is probably because our system goes through the slowly compressing before the crystallization process, which can ensure enough relaxation.

Next, we study the relation between local density and bond-orientational order and their roles played in the crystallization process. In Fig. 6, we plot the transition from the metastable fluid phase to the crystal phase, which has been shown in Fig. 5(a), in the q_6 - ρ plane of the solid bond number ξ (see section 2.2 for its definition, typically, a larger ξ indicates a better crystalline order.) for the state point $T = 0.0052$ and $P = 0.05$. Results for the state point $T = 0.00262$ and $P = 0.01$ are very similar (data not shown). We quantify the correlation of local density and bond-orientational order by using the Spearman rank correlation coefficient $K(\alpha, \beta)$.^{41–43} $K(\alpha, \beta)$ varies from -1 to 1 , with 1 indicating that the two quantities α and β are related by a monotonically increasing function and -1 for the decreasing one. It equals to 0 if the two quantities are uncorrelated. The values of

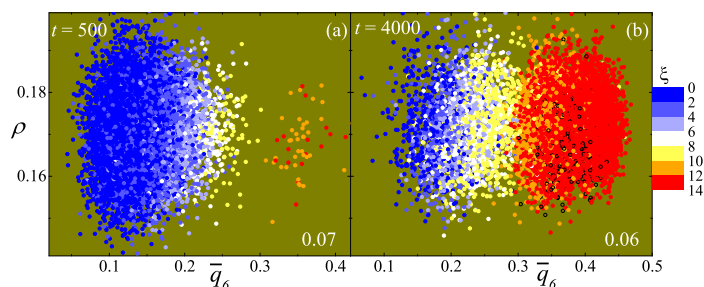


Fig. 7 The solid bond number ξ for all particles of the system in the \bar{q}_6 - ρ plane for the state point $T = 0.0052$ and $P = 0.05$ for $t = 500$ (a) and $t = 4000$ (b). Here, ξ grows from 0 to 14 from the liquid to the crystal phase and is represented by the color of each symbol. Numbers at the lower right indicate Spearman rank correlation coefficients $K(\rho, \bar{q}_6)$, which characterizes the correlation between ρ and \bar{q}_6 .

$K(\rho, q_6)$ are shown in the lower right corner of each histogram in Fig. 6. For the fluid case (see Fig. 6(a)), the value of $K(\rho, q_6)$ is around 0.4 , and this shows positive correlation between local density and bond-orientational order (i.e., the densely packed particles is likely to have relatively large q_6), although this correlation is not strong. The value of $K(\rho, q_6)$ decreases as the crystallization proceeds, indicating that the correlation becomes weak as the growth of the nucleus. This conclusion can also be inferred from the inclination of the distribution of symbols with q_6 axis, since this inclination becomes flatter as crystallization proceeds. This result is consistent with data shown in Fig. 4. Besides, it can be seen that the nucleation starts from the region of high bond-orientational order, but not the densest one (see Figs. 6(b) and 6(c)). These findings are consistent with some recent reports,^{13–16} which are different from the conventional picture of nucleation. Moreover, we have tested the LJ system and obtained similar results (see Fig. S3 in the ESI†). Thus, our findings suggest that it is the bond-orientational order rather than the density that triggers the nucleation process.

However, our above results on the relation between local density and bond-orientational order in the fluid stage is not consistent with the related reports,^{14,15} in which the two quantities uncorrelated with each other has been found. We note that the characterization method of the bond order they used is the coarse-grained form \bar{q}_6 (see Eq. (7)). To investigate whether the characterization methods affect the results, we show in Fig. 7 the solid bond number ξ in the \bar{q}_6 - ρ plane for $t = 500$ and $t = 4000$ at the state point $T = 0.0052$ and $P = 0.05$. Fig. 7(a) and 7(b) give the same state point and same time as Fig. 6(a) and 6(e), respectively. It can be found that \bar{q}_6 can separate solid particles from liquid ones more effectively (see Fig. 7) than q_6 (see Fig. 6). This indicates that \bar{q}_6 is a good determination of the local crystal structure of the system, which is consistent with the work of Lechner and Dellago.³⁶ Different from Fig. 6(a), the distribution of symbols in Fig. 7(a) is almost parallel to the \bar{q}_6 axis and the value of $K(\rho, \bar{q}_6)$ is close to 0 , suggesting that \bar{q}_6 and ρ are uncorrelated with each other even though in the fluid phase.

We show in Fig. 8 the time evolution of the crystal fraction $X = N_{\text{solid}}/N$ and that of the Spearman correlation coefficients $K(\rho, q_6)$ and $K(\rho, \bar{q}_6)$ for the two state points $T = 0.0052$, $P = 0.05$

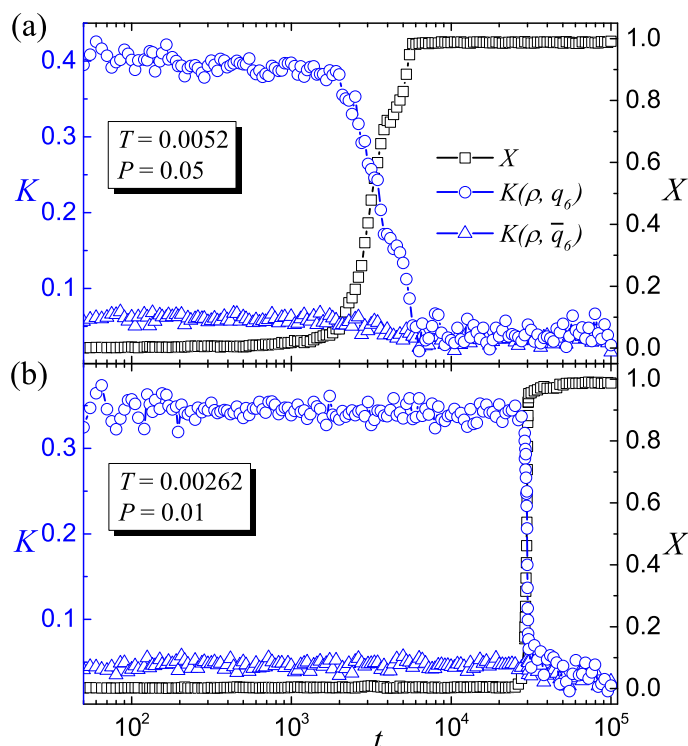


Fig. 8 Time evolution of the crystal fraction $X = N_{solid}/N$ (black squares) and that of the Spearman rank correlation coefficients $K(\rho, q_6)$ (blue circles) and $K(\rho, \bar{q}_6)$ (blue triangles) for the state point $T = 0.0052$ and $P = 0.05$ (a) and the state point $T = 0.00262$ and $P = 0.01$ (b).

and $T = 0.00262$, $P = 0.01$. The curves $K(\rho, q_6)$ and $K(\rho, \bar{q}_6)$ demonstrate different time evolution features for these two state points. $K(\rho, q_6)$ shows clear crystal fraction dependence, i.e., it remains to be a modest value when X is about 0 in the fluid stage and it decreases sharply as increasing X in nucleation and growth stages. Finally, after the crystallization finishes, $K(\rho, q_6)$ goes to ~ 0 . However, $K(\rho, \bar{q}_6)$ remains to be a very small value (close to 0) in the whole crystallization process. Similar results are also obtained for LJ system (see Fig. S4 and the corresponding discussion for more details in the ESI[†]). The different responses of $K(\rho, q_6)$ and $K(\rho, \bar{q}_6)$ to the crystal fraction X reflect that q_6 and \bar{q}_6 characterize differently of the bond-orientational order. From the definition of q_6 and \bar{q}_6 in section 2.2, we can see that they characterize in different spatial scales of the local bond-orientational order. q_6 contains the information of the local structure of the first shell around the target particle, while \bar{q}_6 contains the structural information of the first and the second shells around it. On the other hand, the local density ρ obtained from Voronoi volume only contains the first shell information, which is the same as q_6 . Thus, q_6 is a better quantity to investigate the relation between local density and bond-orientational order because of its matching in spatial scale with ρ . Since the relation between local density and bond-orientational order shows clear crystal fraction dependence, it is suggested that the information of crystal fraction should be contained on investigating this problem.

4 Conclusions

In summary, we present a detailed study of the relationship between local density and bond-orientational order in the crystallization process via MD simulation. We compress the soft particles system, in which particles are interacting via the Gaussian-shaped potential, by increasing the pressure of the system gradually in the isothermal-isobaric ensemble and thus obtain the fluid-solid transition. By investigating the locally dense-packed particles and locally highly bond-orientational ordered particles in the compressing process, we find that the former shows stronger spatial correlation than the latter in the fluid phase, although both correlations are weak. There are sharp increases of the correlations for both of them at the phase transition point, indicating that the first-order phase transition occurs. The spatial correlation of highly bond-orientational ordered particles is larger than that of the densely packed ones in the bcc-favored solid phase and the former is smaller than the latter for fcc-favored solid phase. It indicates that values of these two quantities are affected by crystal structures in the solid phase. Thus, our results indicate the evolution of both density and bond-orientational order in the crystallization process and provide new characterization method of the liquid-crystal transition, i.e., the spatial correlation of locally dense-packed particles and that of the highly bond-orientational ordered particles.

We also focus on the crystallization process at the phase transition point and show that it is bond-orientational order rather than density that triggers the nucleation process. The relationship between local density and bond-orientational order is strongly affected by the characterization methods used. If the bond-orientational order is characterized by q_6 , the correlation between these two quantities shows clear crystal fraction dependence. There is obviously but modestly positive correlation when the crystal fraction is low in the fluid stage. The correlation decreases as increasing the crystal fraction in the nucleation and growth stage. After the crystallization finishes, there is almost no correlation between them. On the other hand, if the bond-orientational order is characterized by the coarse-grained form \bar{q}_6 , we find no correlation between the local density and bond-orientational order in the whole crystallization process. Since the spatial scales of q_6 and ρ are matched, the local density ρ shows stronger correlation with q_6 than with \bar{q}_6 . Nevertheless, \bar{q}_6 , which is originally developed as a more accurate determination of crystal structures compared with q_6 , shows obvious advantage in distinguishing between solid and liquid particles in our work. We should mention that the main conclusions found in this paper are not limited to the Gaussian-core model. We have checked the system with particles interacting via the Lennard-Jones potential, and we can give the similar conclusions (see ESI[†]). Our results also help with clarifying the mechanism of the crystallization process.

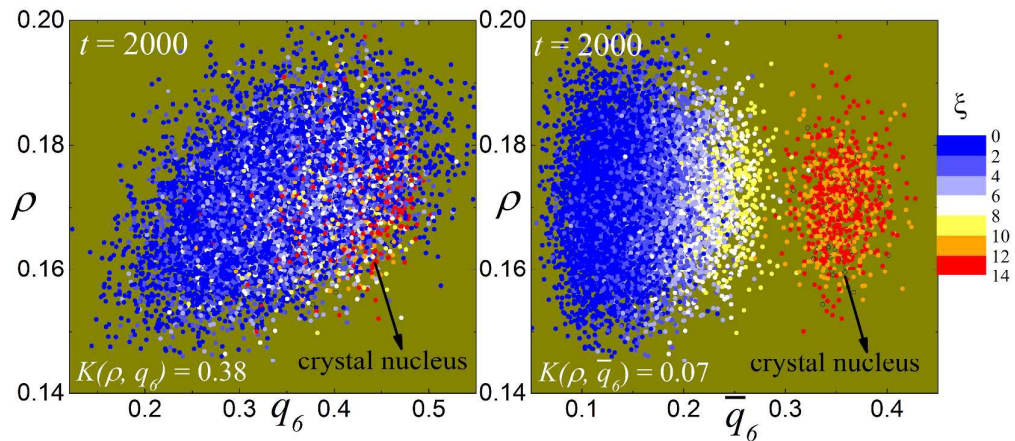
Acknowledgement

We thank Prof. Daan Frenkel, Prof. Hajime Tanaka, Prof. Henri Orland, Prof. Da-Dong Yan, Prof. Wen-Bing Hu and Prof. Paul Chaikin for helpful discussions. This work is subsidized by

the National Basic Research Program of China (973 Program, 2012CB821500), and supported by the National Natural Science Foundation of China (21222407, 21474111) program. The work also forms part of the research programme of the DPI, project No. 779.

References

- 1 K. F. Kelton and A. L. Greer, *Nucleation in Condensed Matter: Applications in Materials and Biology*, Elsevier, Oxford, 2010.
- 2 A. Cacciuto, S. Auer and D. Frenkel, *Nature*, 2004, **428**, 404.
- 3 V. J. Anderson and H. N. W. Lekkerkerker, *Nature*, 2002, **416**, 811.
- 4 R. Becker and W. Döring, *Ann. Phys.*, 1935, **416**, 719.
- 5 P. G. Debenedetti, *Metastable Liquids: Concepts and Principles*, Princeton University Press, Princeton, NJ, 1996.
- 6 P. R. ten Wolde and D. Frenkel, *Science*, 1997, **277**, 1975.
- 7 V. Talanquer and D. W. Oxtoby, *J. Chem. Phys.*, 1998, **109**, 223.
- 8 J. F. Lutsko and G. Nicolis, *Phys. Rev. Lett.*, 2006, **96**, 046102.
- 9 K. G. Soga, J. R. Melrose and R. C. Ball, *J. Chem. Phys.*, 1999, **110**, 2280.
- 10 A. Lomakin, N. Asherie and G. B. Benedek, *Proc. Natl. Acad. Sci. U.S.A.*, 2003, **100**, 10254.
- 11 T. Schilling, H. J. Schöpe, M. Oettel, G. Opletal and I. Snook, *Phys. Rev. Lett.*, 2010, **105**, 025701.
- 12 J. R. Savage and A. D. Dinsmore, *Phys. Rev. Lett.*, 2009, **102**, 198302.
- 13 T. Kawasaki and H. Tanaka, *Proc. Natl. Acad. Sci. U.S.A.*, 2010, **107**, 14036.
- 14 J. Russo and H. Tanaka, *Sci. Rep.*, 2012, **2**, 505.
- 15 P. Tan, N. Xu and L. Xu, *Nat. Phys.*, 2014, **10**, 73.
- 16 K. Kratzer and A. Arnold, *Soft Matter*, 2015, **11**, 2174.
- 17 T. T. Debela, X. D. Wang, Q. P. Cao, Y. H. Lu, D. X. Zhang, H. J. Fecht, H. Tanaka and J. Z. Jiang, *Phys. Rev. B*, 2014, **89**, 104205.
- 18 Y. L. Zhu, H. Liu, Z. W. Li, H. J. Qian, G. Milano and Z. Y. Lu, *J. Comput. Chem.*, 2013, **34**, 2197.
- 19 S. Nosé, *Mol. Phys.*, 1984, **52**, 255.
- 20 W. G. Hoover, *Phys. Rev. A*, 1985, **31**, 1695.
- 21 H. C. Andersen, *J. Chem. Phys.*, 1980, **72**, 2384.
- 22 F. H. Stillinger, *J. Chem. Phys.*, 1976, **65**, 3968.
- 23 F. H. Stillinger and T. A. Weber, *J. Chem. Phys.*, 1978, **68**, 3837.
- 24 F. H. Stillinger and T. A. Weber, *Phys. Rev. B*, 1980, **22**, 3790.
- 25 C. N. Likos, *Soft Matter*, 2006, **2**, 478.
- 26 F. H. Stillinger and D. K. Stillinger, *Phys. A*, 1997, **244**, 358.
- 27 A. Lang, C. N. Likos, M. Watzlawek and H. Löwen, *J. Phys.: Condens. Matter*, 2000, **12**, 5087.
- 28 S. Prestipino, F. Saija and P. V. Giaquinta, *Phys. Rev. E*, 2005, **71**, 050102(R).
- 29 S. Prestipino, F. Saija and P. V. Giaquinta, *J. Chem. Phys.*, 2005, **123**, 144110.
- 30 G. Malescio, *J. Phys.: Condens. Matter*, 2007, **19**, 073101.
- 31 J. Russo and H. Tanaka, *Soft Matter*, 2012, **8**, 4206.
- 32 P. J. Steinhardt, D. R. Nelson and M. Ronchetti, *Phys. Rev. B*, 1983, **28**, 784.
- 33 P. R. ten Wolde, M. J. Ruiz-Montero and D. Frenkel, *J. Chem. Phys.*, 1996, **104**, 9932.
- 34 S. Auer and D. Frenkel, *J. Chem. Phys.*, 2004, **120**, 3015.
- 35 J. L. Finney, *Proc. R. Soc. London, Ser. A*, 1970, **319**, 479.
- 36 W. Lechner and C. Dellago, *J. Chem. Phys.*, 2008, **129**, 114707.
- 37 F. W. Starr, S. Sastry, J. F. Douglas and S. C. Glotzer, *Phys. Rev. Lett.*, 2002, **89**, 125501.
- 38 X. Cheng, *Soft Matter*, 2010, **6**, 2931.
- 39 J. C. Conrad, F. W. Starr and D. A. Weitz, *J. Phys. Chem. B*, 2005, **109**, 21235.
- 40 B. Sun, Z. W. Sun, W. Z. Ouyang and S. H. Xu, *J. Chem. Phys.*, 2014, **140**, 134904.
- 41 C. Sammut and G. I. Webb, *Encyclopedia of Machine Learning*, Springer-Verlag, Berlin, 2011.
- 42 A. Widmer-Cooper and P. Harrowell, *J. Non-Cryst. Solids*, 2006, **352**, 5098.
- 43 G. M. Hocky, D. Coslovich, A. Ikeda and D. R. Reichman, *Phys. Rev. Lett.*, 2014, **113**, 157801.



We find that it is the bond-orientation order rather than local density trigger the nucleation process, and the relation between them is strongly impacted by the characterization methods used.